Facile synthesis of $Cu_2FeSnSe_4$ nanoparticles for solar energy water splitting

X. R. WANG[a], Y. S. GUAN[a], O. A. ALI[b,*], K. F. YAO[a], M. CAO[a,*], J. HUANG[a], L. J. WANG[a], Y. SHEN[a]
[a]*School of Materials Science and Engineering, Shanghai University, Shanghai 200072, China*
[b]*Department of Physics, College of Science, University of Baghdad, Baghdad, Iraq*

Well dispersed $Cu_2FeSnSe_4$ (CFTSe) nanoparticles were first synthesized using the hot-injection method. The structure and phase purity of as-synthesized CFTSe nanoparticles were examined by X-ray diffraction (XRD) and Raman spectroscopy. Their morphological properties were characterized by scanning electron microscopy (SEM) and transmission electron microscopy (TEM). The average particle sizes of the nanoparticles were about 7-10 nm. The band-gap of the as-synthesized CFTS nanoparticles was determined to be about 1.15 eV by ultraviolet-visible (UV-Vis) spectrophotometry. Photoelectrochemical characteristics of CFTSe nanoparticles were also studied, which indicated their potential application in solar energy water splitting.

(Received May 10, 2019; accepted April 9, 2020)

Keywords: Crystal growth, Hot injection, Water splitting

1. Introduction

Over the past several years, ternary and multinary semiconducting compounds have attracted great interest for their physical properties and their potential technological applications [1,2]. Among these, Cu_2ZnSnS_4 (CZTS), Cu_2FeSnS_4 (CFTS), $Cu_2ZnSnSe_4$ (CZTSe) and $Cu_2FeSnSe_4$ (CFTSe) have received much attention due to their earth-abundant composition and similar structure with that of $CuInGaSe_2$ (CIGSe) [3-6]. The highest power conversion efficiency of CZTS-based solar cells has beyond 11 % [7]. As quaternary semiconductor material, CFTSe has also been studied as an alternative due to its optimal band gap (~1.5 eV), high absorption coefficient ($>10^4$ cm^{-1}) and earth-abundant elements. However, the photoelectrochemical properties of CFTSe nanoparticles remain largely unexplored.

High quality copper based quaternary compound thin films are usually fabricated by physical methods, such as sputtering, thermal evaporation, pulsed laser deposition and so on [8-10]. But these methods need high cost and complicated devices, which will hinder their widely application on photoelectric devices. A hydrothermal method has previously been utilized to synthesize CFTSe nanosheets [11,12]. However, the dispersion of the as-synthesized CFTSe nanoparticles is not very good and their particles sizes are also not well controlled. The present paper is the first to report on the synthesis of CFTSe nanocrystals using the hot-injection method, which can synthesize size controlled CFTSe nanopartilces with good dispersivities. It will play a key role in the low cost and large-scale fabrication of photoelectric devices.

The present study investigated the growth process of CFTSe nanoparticles and identified the intermediates. The structural, morphological, and optical properties of CFTSe nanoparticles were investigated. These nanocrystals can be easily dispersed in relatively low toxic solvents and they can be well fabricated into CFTSe films by drop-casting. The photoelectrochemical response of the obtained film was also evaluated. Thus, the present study contributes to advancing the photoelectric device applications of CFTSe nanocrystals.

2. Experiments

2.1. Materials

Copper (II) chloride dihydrate ($CuCl_2 \cdot 2H_2O$), Iron (II) chloride ($FeCl_2$), tin (IV) tetrachloride pentahydrate ($SnCl_4 \cdot 5H_2O$), selenium powder, diketopyrrolopyrrole (DPP) and oleylamine (OLA) were purchased from J&K.

2.2. Preparations

In a typical synthesis, a mixture of 0.2 mmol $CuCl_2 \cdot 2H_2O$, 0.1 mmol $FeCl_2$, 0.1 mmol$SnCl_4 \cdot 5H_2O$, and 10 ml OLA were dissolved in a three-neck bottle under the protection of an argon (Ar) atmosphere. The solution was magnetically stirred and heated to 280°C. Next, 0.4 mmol selenium powder was dispersed in 5 ml DDP to form the DPP-Se complex in a glove box. At the reaction temperature of 280°C, 5 ml DPP-Se was injected into the three-neck bottle and kept for 5 minutes. After reaction, the CFTSe nanoparticles were centrifuged using alcohol and toluene. The CFTSe nanoparticles were sprayed onto fluorine doped tin oxide (FTO) substrates, and then a 15 nm CdS layer was deposited onto the CFTSe thin film using the chemical bath deposition method. A solution containing 34 ml deionized water, 5 ml $CdSO_4$ (0.025 mM), 6.52 ml NH_4OH (0.17 M) and 5 ml $CS(NH_2)_2$ (3.24 mM) were used in the CBD process, which was carried out at 60 C for 10 min. Finally, a 5 nm platinum (Pt) electrode layer was sputtered onto the surface of the CdS thin film (Baltec 500).

2.3. Characterizations

The microstructures and the crystals of the as-prepared samples were characterized using X-ray diffraction (XRD) (RigakuD/max 220 kV); Raman (JY-H800UV) spectroscopy was used to examine the phase purities of the CFTSe nanoparticles. An ultraviolet-visible (UV-vis) spectrophotometer (Jasco UV-570) was used to study the optical properties of the CFTSe nanoparticles. The morphological properties of the CFTSe nanoparticles were characterized by scanning electron microscopy (SEM) (FEI Sirion 200) and transmission electron microscopy (TEM) (JEOL 2010 F). The valance states of the elements from CFTSe were examined by X-ray photoelectron spectroscopy (XPS, ESCALAB250Xi). The photocurrent-time response of the CFTSe thin films was tested in 0.5M Na_2SO_4 (pH=0.5) under a light source with 100 mW/cm^2 (AM 1.5 G). FTO/CFTSe, FTO/CFTSe/Pt and FTO/CFTSe/CdS/Pt were used as the working electrodes. Ag/AgCl was used as the reference electrode.

3. Results and discussion

3.1. Synthesis of CFTSe nanoparticles

Fig. 1(a) shows the XRD patterns of the as-synthesized CFTSe nanoparticles. Obvious diffraction peaks appear at 27.17°, 45.07°, 53.41°, 65.65°, 72.41° and 83.22°, which correspond to the (112), (204), (116), (400), (316) and (422) planes of the tetragonal structured CFTSe (PDF No. 27-0167). According to the full width of half maximum (FWHM) values of the (112) diffraction peak, their average grain sizes are estimated to be about 10 nm. It is known that the crystal structure of Cu2SnSe3 and Cu2Se is very similar to that of CFTSe. Thus, Raman characterizations were performed to examine the phase purity of the CFTSe nanoparticle thin films. Three obvious peaks appeared at 209 cm^{-1}, 267 cm^{-1}, and 378 cm^{-1}, confirming the main products of CFTSe. No Raman peaks were found at 180 cm^{-1}, 236 cm^{-1}, 251 cm^{-1}, and 260 cm^{-1}, which indicates that no secondary phase, such as Cu_2SnSe_3, CuSe, and Cu_2Se, exists [13-15] as shown in Fig. 1(b).

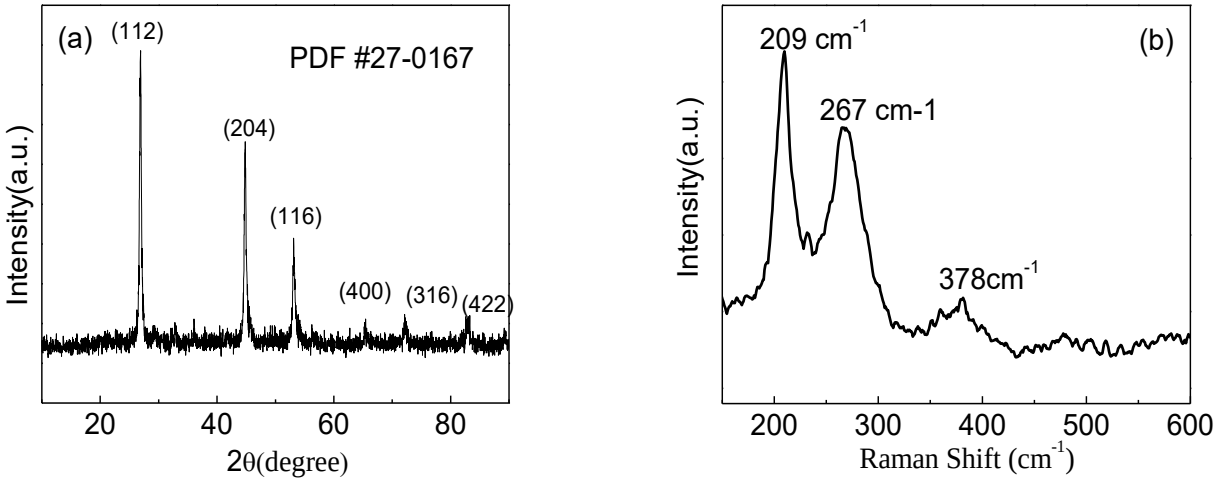

Fig. 1. XRD (a) and Raman (b) spectra of CFTSe nanoparticles

The as-synthesized CFTSe nanoparticles were dip-coated onto the FTO substrates, and the surface properties were characterized by SEM. As shown in Fig. 2(a), the surface of the CFTSe thin films is very compact and it is composed of small nanoparticles. The energy dispersive spectroscopy (EDS) measurements indicate that the atomic compositional ratio of the CFTSe nanoparticles is 20.1:12.2:13.4:54.3, which is close to the theoretical value of 2:1:1:4. The transmission electron microscopy (TEM) characterizations indicate that the CFTSe nanoparticles have uniform average sizes, which are about 8-10 nm, and this finding agrees well with the values calculated by XRD. In the high-resolution transmission electron microscopy (HRTEM) image, the interplanar spacing of 2.01 Å corresponds to the (220) planes of the CFTSe sheets. The diffraction spot of the (111) plane in the selected area electron diffraction (SAED) image indicates the single crystal nature of the CFTSe nanoparticles.

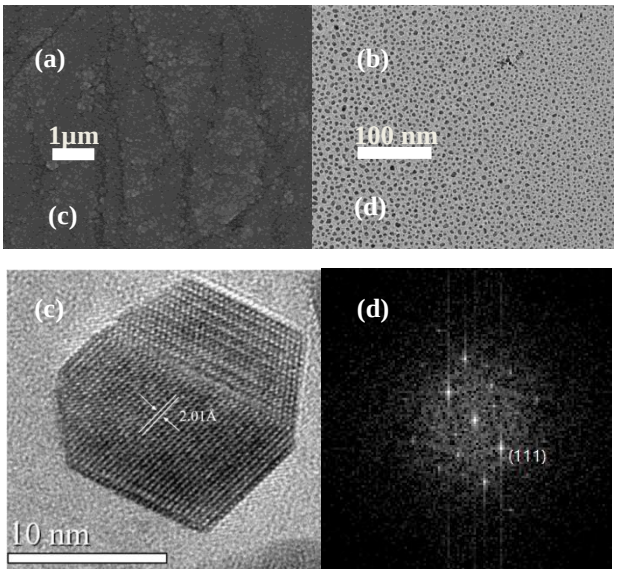

Fig. 2. SEM (a), TEM (b), HRTEM (c) and the corresponded SAED pattern (d) of CFTSe nanoparticles

The CFTSe nanoparticles were dispersed in chloroform and their absorption spectra are presented in Fig. 3. As shown, the CFTSe nanoparticles have obvious absorption in the visible light range, and their bandgaps are determined to be approximately 1.15 eV, according to Equation 1 [16,17]:

$$(ahv)^2=A(hv-E_g) \quad (1)$$

where a is the absorption coefficient, A is a proportional constant, and E_g is the band-gap energy. The valence states of the elements in CFTSe nanoparticles were analyzed by XPS, as shown in Fig. 4. XPS spectrum of Cu (I) show two peaks at 932.3 and 952.1 eV with a peak splitting of 19.8 eV. The satellite peak of iron is too strong, which leads to that the iron $2p_{3/2}$ at 707.6 eV is not so obviously. The tin $3d_{5/2}$ and $3d_{3/2}$ peaks at 486.1 and 494.5 eV, which have a a peak splitting of 8.4 eV and agree well with that of Sn (IV). The binding energy of Se $3d_{5/2}$ peak at 54.1 eV corresponds to that of Se[2]. Our reports agree well with previous studies [11].

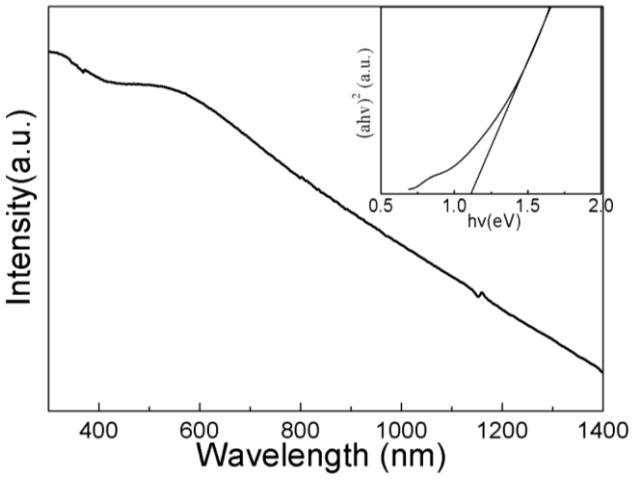

Fig. 3. Absorption spectra of CFTSe nanoparticles and the insect shows the calculated bandgaps

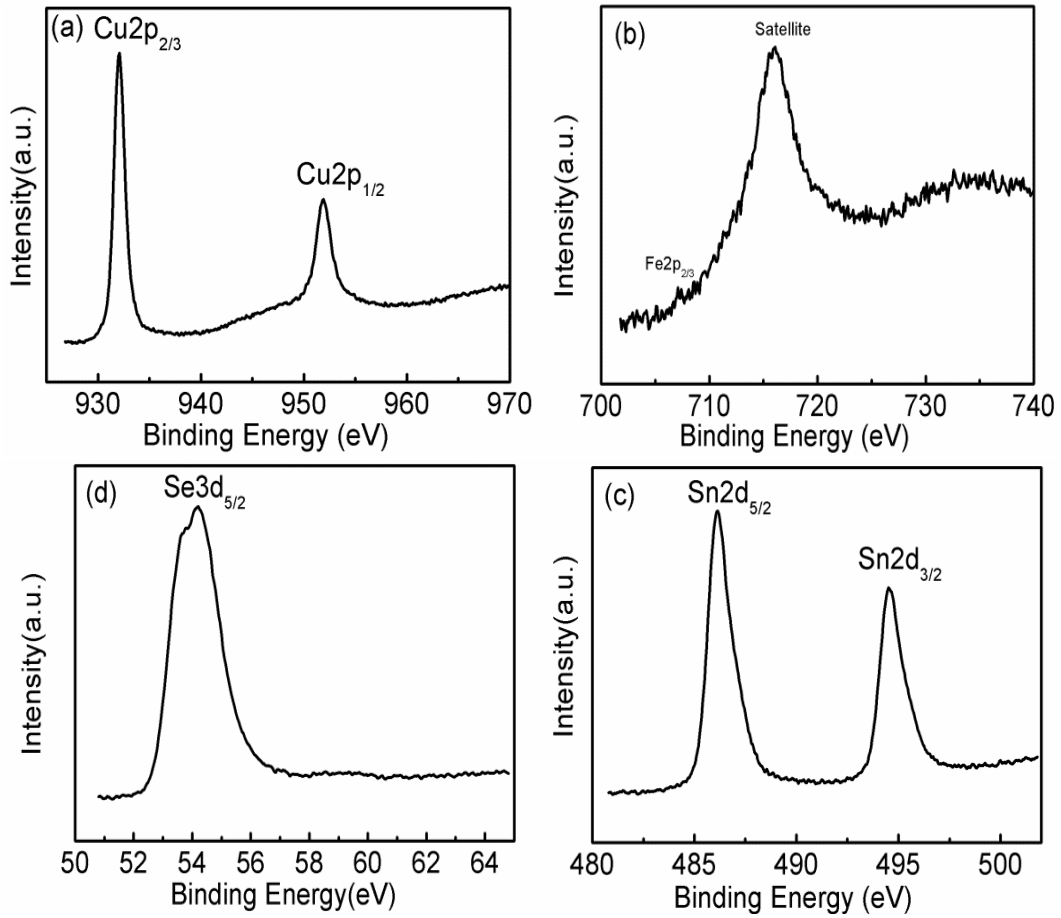

Fig. 4. XPS characterization of CFTSe nanoparticles: Cu 2p (a), Fe 2p (b), Sn 3d (c), Se 3d (d)

PEC responses of FTO/CFTSe thin films were studied under chopped light illumination condition. In Fig. 5a, the cathodic potential is scanned from -0.4 to 0 V and the current-potential curves are decreased gradually, which indicates that p-type CFTSe thin films have been deposited. The deposition of Pt thin films onto the surface of CFTSe films can enhance its catalysis characteristics [18]. And deposition of n-type CdS thin films will form a p-n junction with CFTSe, which can also separate the photogenerated charge carriers efficiently [19]. All of these are confirmed by the current-potential curves in Fig. 5a. From the current-time curves in Fig. 5b, the photocurrent densities of FTO/CFTSe are about 9 μA/cm^2. After depositing of CdS and Pt thin films, the photocurrent density of FTO/CFTSe/Pt and FTO/CFTSe/CdS/ Pt thin films were increased to 15 and 38 μA/cm^2, respectively. The fabrication of FTO/CFTSe/CdS/Pt can enhance the photoelectrochemical properties of FTO/CFTSe greatly.

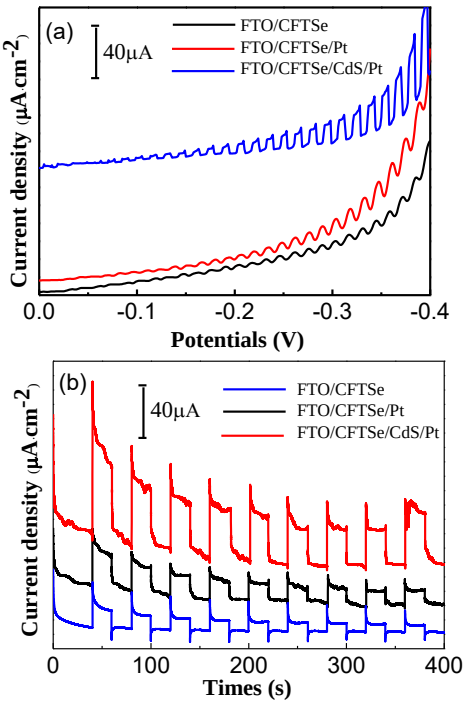

Fig. 5. I-V (a) and I-t (b) curves of FTO/CFTSe, FTO/CFTSe/Pt and FTO/CFTSe /CdS/Pt (color online)

4. Conclusions

In conclusion, CFTSe nanoparticles were prepared by a convenient hot-injection method for the first time. The as-synthesized CFTSe nanoparticles were well dispersed and the averaged particles sizes are about 10 nm. From the optical absorption spectra, the band-gap of CFTSe nanoparticles was estimated to be about 1.15 eV. The fabrication of FTO/CFTSe/CdS/Pt enhanced the photoelectrochemical properties of FTO/CFTSe greatly, which is contributive to the development of CFTSe nanoparticles on solar energy water splitting.

Acknowledgements

We acknowledge Instrumental Analysis & Research Center of Shanghai University for the help of characterization works.

References

[1] C. Schubbert, P. Eraerds, M. Richter, J. Parisi, I. Riedel, T. Dalibor, J. Palm, Sol. Energ. Mater. Sol. C **157**, 146 (2016).
[2] Y. C. Lin, D. H. Hong, Y. T. Hsieh, L. C. Wang, H. R. Hsu, Sol. Energ. Mater. Sol. C **155**, 226 (2016).
[3] C. Yan, C. Huang, J. Yang, F. Y. Liu, J. Liu, Y. Q. Lai, J. Li, Y. X. Liu, Chem. Commun. **48**, 2603 (2012).
[4] X. Y. Zhang, N. Z. Bao, K. Ramasamy, Y. H. A. Wang, Y. F. Wang, B. P. Lin, A. Gupt, Chem. Commun. **48**, 4956 (2012).
[5] R. H. Zhang, S. M. Szczepaniak, N. J. Carter, C. A. Handwerker, R. Agrawal, Chem. Mater. **27**, 2114 (2015).
[6] P. M. P. Salome, P. A. Fernandes, A. F. da Cunha, J. P. Leitao, J. Malaquias, A. Weber, J. C. Gonzalez, M. I. N. da Silva, Sol. Energ. Mater. Sol. C **94**, 2176 (2010).
[7] T. K. Todorov, J. Tang, S. Bag, O. Gunawan, T. Gokmen, Y. Zhu, D. B. Mitzi, Adv. Energy Mater. **3**, 34 (2013).
[8] R. Nakamura, K. Tanaka, H. Uchiki, K. Jimbo, T. Washio, H. Katagiri, Jpn. J. Appl. Phys. **53**, 02BC10 (2014).
[9] C. W. Shi, G. Y. Shi, Z. Chen, P. F. Yang, M. Yao, Mater. Lett. **73**, 89 (2012).
[10] W. J. Baumgardner, J. J. Choi, K. F. Bian, L. Fitting Kourkoutis, D. M. Smilgies, M. O. Thompson, T. Hanrath, ACS Nano **5**, 7010 (2011).
[11] M. Cao, B. L. Zhang, J. Huang, Y. Sun, L. J. Wang, Y. Shen, Chem. Phys. Lett. **604**, 15 (2014).
[12] B. L. Zhang, M. Cao, L. Li, Y. Sun, Y. Shen, L. J. Wang, Mater. Lett. **93**, 111 (2013).
[13] G. Marcano, C. Rincón, S. A. López, G. S. Pérez, J. G. Alvarez, Solid State Commun. **151**, 84 (2011).
[14] V. I. Roca, E. Saucedo, C. M. Ruiz, X. Fontané, L. C. Barrio, V. Bermudez, Phys. Status Solidi A **206**, 1001 (2009).
[15] V. I. Roca, A. P. Rodríguez, A. R. Rodríguez, J. R. Morante, J. Á. García, J. Appl. Phys. **101**, 103517 (2007).
[16] M. Ikhlasul Amal, Kyoo Ho Kim, J. Mater. Sci.: Mater. Electron. **24**, 559 (2013).
[17] F. Luckert, D. I. Hamilton, M. V. Yakushev, N. S. Beattie, G. Zoppi, M. Moynihan, I. Forbes, A. V. Karotki, A. V. Mudryi, M. Grossberg, J. Krustok, R. W. Martin, Appl. Phys. Lett. **99**, 062104 (2011).
[18] X. L. Yu, A. Shavel, X. Q. An, Z. S. Luo, M. Ibańez, A. Cabot, J. Am. Chem. Soc. **136**, 9236 (2014).
[19] W. Cheng, N. Singh, W. Elliott, J. Lee, A. Rassoolkhani, X. J. Jin, E. W. McFarland, S. Mubeen, Adv. Sci. **5**,1700362 (2017).

*Corresponding author: caomeng@shu.edu.cn;
omarlibra2005@yahoo.com